redin Revista Facultad de Ingeniería, Universidad de Antioquia, No. 78, pp. 99-104, 2016

Spectral-amplitude encoding CDMA system based on high-speed electronic encoder/ decoder structures

UNIVERSIDAD DE ANTIOQUIA 1803

Sistema de codificación CDMA de amplitud de sub-bandas basado en estructuras de codificación/ decodificación electrónica de alta velocidad

Jorge Aguilar-Torrentera*, Jesús Ramón Rodríguez-Cruz, Norma Patricia Puente-Ramírez, Gustavo Rodríguez-Morales

Universidad Autónoma de Nuevo León, Facultad de Ingeniería Mecánica y Eléctrica. Av. Universidad s/n, Ciudad Universitaria, San Nicolás de los Garza. C. P. 66455. Nuevo León, México.

ARTICLE INFO

Received March 02, 2015
Accepted October 01, 2015

KEYWORDS

Optical fiber CDMA, spectral encoding, multi-Gbps networks, transversal filter, distributed amplifier, user orthogonality

CDMA de fibra óptica, codificación espectral, Redes a velocidades de multi-Gbit/s, filtro transversal, amplificador distribuido, ortogonalidad

ABSTRACT: A new method for high-speed Code Division Multiple Access (CDMA) systems that lies on the analogue performance of distributed-based transversal filters is proposed. The method allows spectral-amplitude encoding CDMA system implementations leading to an improvement of orthogonality among users over temporal encoding direct-sequence systems. The maximal degrees of flexibility in the design of transversal filters are considered to generate waveforms that exhibit large temporal variation over the filter span time in accordance with an encoded waveform. Applications of our method to high-speed CDMA are discussed towards the end of the paper.

RESUMEN: En este artículo se propone un método nuevo para sistemas de multi-canalización por división de código (CDMA, por sus siglas en inglés) para sistemas de alta velocidad, el cual radica en el desempeño analógico de filtros transversales distribuidos. El método permite el diseño de sistemas de codificación de amplitud de sub-bandas CDMA, el cual presenta un mejor desempeño en comparación con aquel que se obtiene al utilizar codificación temporal de secuencia directa. Se considera la máxima flexibilidad en el diseño de filtros transversales para obtener una variación temporal amplia de las formas de onda que se propagan lo largo de la línea de retardo del filtro transversal de acuerdo a una señal codificada espectralmente. Aplicaciones del método a las redes CDMA de alta velocidad se discuten al final del artículo.

1. Introduction

For the past years, there have been major advances in the enabling technology for deploying all-optical networks in which the associated transport and processing functions remain entirely in the optical domain. In the field of Optical Code Division Multiple Access (OCDMA), multi-Gbps networks encompass different functions mainly relying on optical devices to encode and decode user data. Coherent and non-coherent encoding schemes have been proposed by making use of the methods of modulation and detection used in fiber optic communication systems. However the development of OCDMA networks at a wide scale is yet incomplete mainly owing to the high-cost incurred in their deployment [1]. In fairly recent developments, the electronic processing of codes employing distributed-based transversal filters (DTF's) [2, 3] has been considered as a technique to employ in multi-Gbps asynchronous networks. Besides the low-cost incurred in its deployment, the electronic technique avoids optical losses featured in optical matched filters and it relies on optical devices solely for transport functions and signal distribution.

Hitherto, the DTF has been used to generate and correlate high-rate binary sequences in direct sequence (DS)-CDMA systems. Early work on the filter method confirmed the practicality of symbol-rate DTF design by achieving zero inter-symbol interference (ISI) in the reception of high-rate sequences [4]. In other proposal, time-domain encoding of unipolar pulses was considered in [3] as a method by which code is impressed on variable delays between consecutive pulses. Nonetheless, the span time of the filter taped delay line is highly constrained by filter design considerations. Therefore the distance between consecutive pulses becomes low preventing from keeping low cross-correlation parameters in the reception of CDMA signals as more users are added in the network.

The first practical demonstration of multi-Gchips/s electronic CDMA system for optical access networks

* Corresponding author: Jorge Aguilar Torrentera
e-mail: jorge.aguilart@uanl.mx
ISSN 0120-6230
e-ISSN 2422-2844

DOI: 10.17533/udea.redin.n78a13

was reported in [2]. Fractionally-spaced transversal filters featuring a tap gain tuning capability were used to generate encoding patterns with compensated inter-pulse interference. User data is decoded by obtaining a correlation pulse in the intended node receiver and comparing its amplitude against a threshold level. Threshold electronics can work at speeds compatible with the synchronous operation of the transversal filter (at multi-Gchip/s). Nonetheless, the large side-lobe cross-correlation output that results from using quasi-orthogonal codes prevents from increasing the number of simultaneous users in the network without deteriorating performance. More recently, an electro-optic encoder/decoder structure in which each electronically encoded chip modulates a slot or frequency bin to form a spectrally encoded CDMA signal was proposed [5]. Nonetheless, the structure requires intensity modulators and a large number of optical devices which makes the electro-optic approach costly for a network developed at a wide scale.

From the above, it is apparent that a straightforward adaptation of the previously proposed encoding methods to the electronic processing of codes via the DTF method leads to significant limitations in the development of CDMA networks. In this paper, new filter structures for use in spectral-amplitude encoding CDMA systems are introduced. Our proposal is motivated by early work on OCDMA based on spectral encoding of non-coherent sources [6] in which multiple-user interference is cancelled out by balanced detection of spectrally encoded pulses. It is found that the transient characteristics of DTF's are appropriate to synthesize spectrally-encoded waveforms based on the Spread Time (ST) technique [7]. It is well-known that in order to keep orthogonality among users, encoder and decoder functions have to extend beyond the symbol interval. Such a pulse spread is aimed to ensure minimal overlap between neighboring frequency slots of the assigned waveforms. Although the filter approach based on distributed amplifier principles can produce a variety of high-rate pulse filtering functions [8] the synthesis of spread-in-time signals by DTF's requiring more than 7 or 8 taps is prohibitive due to filter losses and size constrains. In the proposed method, pulse responses are mostly spread over the filter span time, *T*, by taking advantage of the low degradation of the rise time parameter of distributed filter stages. To approximate CDMA functions, waveforms are truncated with a square pulse of width equal to the filter time span. As a consequence, the ensuing spectrum consists of a number of sub-bands bearing both code information and interference; the latter is introduced in the form of sub-band side-lobes spread over the available bandwidth. The encoder/decoder structures herein proposed can reduce sub-band interference by a careful selection of filter functions. Our method is appraised by showing that encoder and decoder functions with spectral content depending on orthogonal codes result in suitable matched filtering and multi-user interference rejection capabilities.

2. CDMA method

A scheme of the proposed CDMA system based on filter structures is illustrated in Figure 1. Each filter function is synthesized by a finite-impulse response (FIR) that requires processing short pulses comprising variable delay between consecutive pulses and multilevel pulse weighting. For such aim, the DTF as a signal processor that presents the maximal degree of freedom in the design [8] is adopted. The filter function is given by Eq. (1).

$$h(t)=w(t)\sum_{n=1}^{M}c_n\cos(\omega_n t-\varphi_n) \tag{1}$$

where $\omega_n=2\pi n/T$, M is the number of sub-bands, $w(t)$ is a time window function, $w(t)=1;\ 0<t\le T$, and $w(t)=0;$ elsewhere. For brevity, ϕ_n and c_n are referred to as the phase and the amplitude of the nth-subband, respectively. The sub-bands are separated by $1/T$ [Hz] away from side-lobe centers and each sub-band amplitude and phase are modulated to encode and decode data.

The scheme of the proposed CDMA system in Figure 1 is described as follows. Each information bit is encoded by a waveform that conveys code information in sub-band amplitudes $(c_1,c_2,...,c_n)$. At the decoder, input power is split to correlate with two functions. Briefly speaking, the correlation output of each filter consists of a number of sub-bands modulated by the amplitudes and phases of the corresponding filter function. At the upper branch, the correlator function provides address information in the phase vector ϕ.The lower-branch function, which is made available to all decoders, shifts the phases of input sub-bands by the vector $\theta=(\theta_1,\theta_2,...,\theta_n)$. In the lower-branch function all sub-band amplitudes are set to one and the output produces a reference with which the user correlated spectrum is mixed to produce a new sub-band with spectral content within the lowpass filter bandwidth. The bandwidth requirements are equal to the bit-rate.

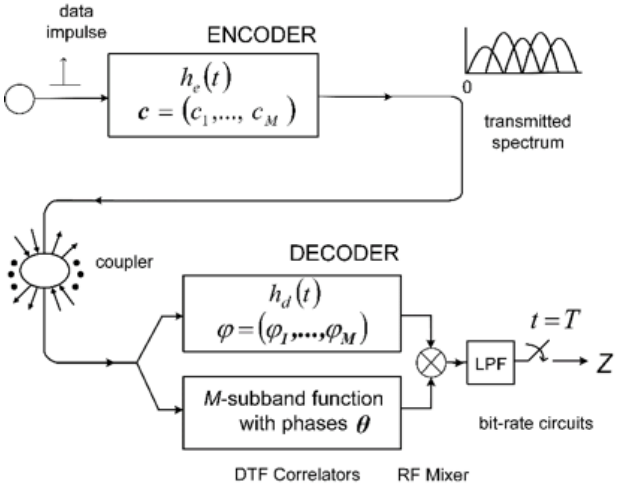

Figure 1 CDMA scheme showing an encoder/decoder pair. Impulse functions are synthesized by DTF's pulse responses

A receiver with address $\left(\phi_1^y,\phi_2^y,...,\phi_M^y\right)$ will produce the output as the summation given by Eq. (2).

$$Z=\sum_{n=1}^{M}c_n^2 cos\left(\varphi_n^y-\theta_n\right) \tag{2}$$

Since the amplitude of each user sub-band is square raised and user phases are cancelled out in the demodulation process the receiver can retain only user power. As a consequence encoding functions are constrained to be positive. Code constructions initially proposed for spectral-amplitude encoding OCDMA systems [6] are herein considered to achieve perfect orthogonality among users. When testing with binary codes, the receiver address function have sub-band amplitudes set to one and the phase differences $\phi_q^y-\theta_q$ are chosen from $\{0,\pi\}$ for $q=1,..,M$.

3. Filter design method

A design method for FIR-based encoder and decoder filters is introduced. Consider a user encoded with $\left(c_1,c_2,...,c_n\right)$ sub-band phases set to the vector $\left(\beta_1,\beta_2,...,\beta_n\right)$ and a decoder function depending on the phase vector $\left(\phi_1,\phi_2,...,\phi_n\right)$. Eq. (3) is the receiver correlation function that comprises the most significant terms and given by:

$$\begin{aligned} z_\varphi(t)&=\frac{1}{2}\sum_{n=1}^{M}c_n p(t)cos\left(\omega_n t-\Delta_{n,n}^{\varphi}\right)\\ &\quad+\frac{T}{4\pi}\sum_{k=1}^{M}\sum_{l=1,l\neq k}^{M}\mu_{k,l}^{\varphi}(t)-\mu_{k,l}^{\varphi}(t-T),\\ \mu_{k,l}^{\varphi}(t)&=c_k w(t)\left(sin\left(\omega_k t-\Delta_{k,l}^{\varphi}\right)-sin\left(\omega_l t-\Delta_{k,l}^{\varphi}\right)\right)/\,k-l \end{aligned} \tag{3}$$

where $p(t)=w(t)\otimes w(t)$, '$\otimes$' denotes convolution and $\Delta_{k,l}^{\phi}$ is equal to $\beta_k-\phi_l$. The correlation output of the lower branch, $z_\theta(t)$, and its derived function $\mu_{k,l}^{\theta}(t)$ have similar equations just need to substitute $\Delta_{k,l}^{\phi}$ by $\Delta_{k,l}^{\theta}$ into Eq. (3). The first term is the correlation contribution between frequency-aligned sub-band main-lobes of encoder/decoder functions. In the second term, $\mu_{k,l}^{\phi}(t)$ accounts for the correlation contribution between encoder/decoder functions with sub-band side-lobes extending over frequencies that overlap with main-lobe portions thus representing sub-band interference. Chief among interference products, $\mu_{k,k+1}^{\phi}(t)$ result in the larger interference; according to Eq. (3).

A filter design method is introduced to reduce the effect of frequency overlap so that much of the pulse energy at the output is due to the demodulation process of frequency aligned sub-band main-lobes. The mixing between both filter correlation outputs not only involves frequency-aligned correlated sub-bands but also the cross-term products $p(t)cos\left(\omega_n t-\Delta_{n,n}^{\phi}\right)\left(\mu_{k,l}^{\theta}(t)-\mu_{k,l}^{\theta}(t-T)\right)$ and $p(t)cos\left(\omega_n t-\Delta_{n,n}^{\theta}\right)\left(\mu_{k,l}^{\phi}(t)-\mu_{k,l}^{\phi}(t-T)\right)$. At first sight, for sinusoids of main-lobes and interfering side-lobe products of same frequency, unwanted sub-bands will fall into the lowpass filter bandwidth creating potential interference. A straightforward examination however shows that interference created by some cross products can be filtered out of the receiver output by a proper choice of phases. In order to create a number of orthogonal channels, all encoders and decoders are fixed to the phase vector $\theta=\left(\theta_1,\theta_2,...,\theta_n\right)$ to generate a reference at the decoders to mix with the (address) correlator output. By this means, each decoder can be set with a unique phase address. Now, to reduce sub-band interference, a choice of phases $\Delta_{k,k+1}^{\phi}$ and $\Delta_{k,k+1}^{\theta}$ from $\{\pi/2,-\pi/2\}$ for $q=1,..,M-1$ makes the interfering cross-products odd functions about T, resulting in a smaller interfering signal at the receiver output. The above phase selections lead to fix $\theta=\left(\theta_1,\theta_2,...,\theta_n\right)$ to the alternate sequence vector $\left(0,\pi/2,0,\pi/2,...\right)$.

4. Results

In order to test the CDMA method unipolar and bipolar versions of Hadamard codes of length 4 are used. Table 1 shows mutually orthogonal codes and also itemizes the corresponding sub-band phases referred to the alternate vector $\theta=\left(\pi/2,0,\pi/2,0\right)$ to achieve zero cross-correlation, according with Eq. (2). The codework containing all 1's cannot be considered since a user depending on this code has different power from the rest, which have the same number of 1's and 0's.

Table 1 Hadamard codes of length 4. Code phase column is referred to the fixed vector θ=(π/2,0,π/2,0).

Hadamard code	Unipolar code, c	Code phase, φ
(1,1,1,1)	(1,1,1,1)	(π/2, 0, π/2, 0)
(−1,−1,1,1)	(0,0,1,1)	(−π/2, π, π/2, 0)
(1,−1,−1,1)	(1,0,0,1)	(π/2, π, −π/2, 0)
(−1,1,−1,1)	(0,1,0,1)	(−π/2, 0, −π/2, 0)

According with the filter method, waveform design needs a selection of phases uniformly spaced on the unit circle such as $\pm\pi/2$, 0 and π. However, this selection is arbitrary since the receiver output is phase-invariant and therefore a phase shift can be applied to all encoder/decoder functions with the aim to reduce inaccuracies in the synthesis.

The main source of discrepancies are associated with the rise time of practical DTF's, which is constrained by the filter bandwidth (and approximately equal to the inverse reciprocal of the input pulse width) making the DTF response unable to keep up the large variation of some target signals truncated with a rectangular pulse. This point will be highlighted in a following section.

To test the CDMA scheme, DTF's were designed using the filter topology previously reported in [4, 9] and designed by allowing the DTF to have different inter-stage delay and gain weights, according to a target signal. Code dictates filter design parameters. Figure 2 represents the DTF as a signal processor that affords the maximal flexibility. In practical filters, broadband delay structures coupled to distributed gain cells were designed to provide the necessary inter-stage delay. However, some time mismatch is expected since each constituent stage of a delay line is designed to feature a finite time delay resolution therefore the required analogue delay time is obtained approximately by cascading delay stages.

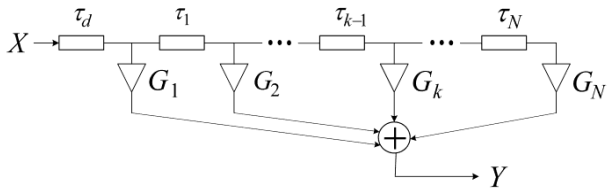

Figure 2 Block diagram representing DTF's structures, where inter-stage delay and tap gains are optimized for CDMA signal synthesis

Artificial transmission lines are designed to show linear phase within the filter bandwidth (approximately equal to a half of the Bragg cut-off frequency). Input pulses of some tens of picoseconds undergo low dispersion and distortion effects as they travel down on artificial transmission lines.

Figure 3 shows pulse transient responses of an 8-tap DTF obtained by adjusting separately a given filter tap to the maximum gain and the remaining tap weights are set to zero. Those are simulation results based on Advanced Design System (ADSTM). Full electromagnetic simulation accounting for coupling among the different monolithic microwave integrated circuits, (MMIC) elements and this was done by MOMENTUMTM. Those correspond to filter implementations with uniformly spaced stages. delay time was set to be equal to 25 ps. It shows that the width of pulses traveling at different filter paths will increase to such a level that tails from adjacent pulses interfere. High-frequency oscillations arise owing to multiple reflections in filter stages. Such effects are taken into consideration for DTF's designs with different inter-stage delays and gain weights.

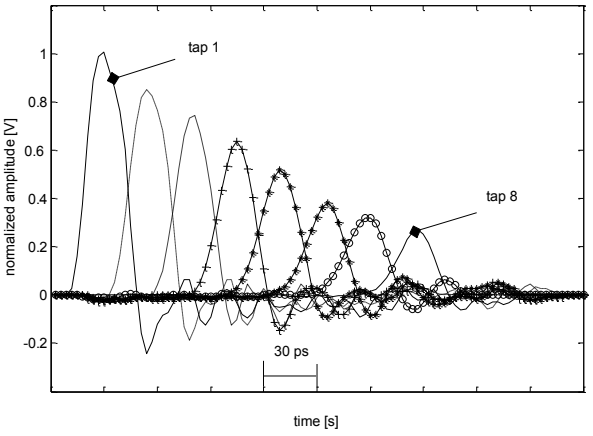

Figure 3 Pulse responses of a filter with uniform inter-stage delay of 25 ps and normalized to the maximal output pulse amplitude

Tap gain adjustment allows compensating attenuation, pulse broadening and high-frequency oscillations within the filter span time. Based on the resulting tap transient responses, algorithms were developed to help in optimizing filter responses.

It is important to mention that by making the first sub-band equal to zero; $c_1 = 0$ and $M = 5$ in Eq. (1), sub-band interference rejection is improved. In the following, the first sub-band amplitude coefficient was made equal to zero in all DTF functions and ϕ_1 is equal to zero to complete the phase vector in Eq. (1).

Figure 4 shows the transient responses of a 7-tap DTF (waveform normalized with its root mean square, r.m.s.) which was synthesized to perform the reference correlation function. Time and amplitude mismatches between the DTF function (simulated reference) and the reference function are noticed. The designed waveform displays a large oscillation beyond the symbol interval.

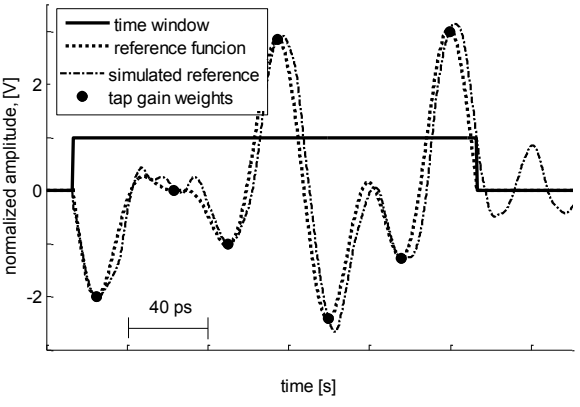

Figure 4 Pulse response of a 7-tap DTF used as reference with c=(0,1,1,1) and Θ=(0, π/2,0, π/2,0).

Figure 5 displays encoder and decoder functions using the filter synthesis. It shows the waveforms of the encoder (0,0,1,0,1) and the (orthogonal) decoder $(0,\pi/2, \pi,-\pi/2, 0)$. Regarding the simulated decoder, it is seen that much of its

energy is kept within the time window. Figure 5 also allows contrasting the encoder function and the corresponding DTF response; it exhibits large discrepancies at both edges of the time-window. In fact, the analogue performance of this address function leads to the worst decoding performance among the other receivers. It is seen that time truncation of the ideal decoder function needs for synthesizing initial and late taps of the DTF with high gains leading necessarily to inaccuracies owing to a large pulse spread beyond the symbol interval.

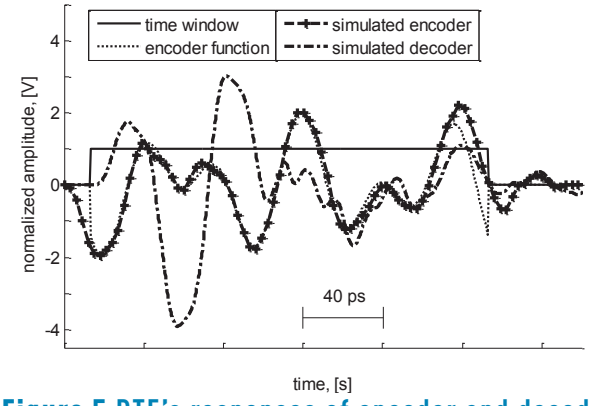

Figure 5 DTF's responses of encoder and decoder functions based on the codes c=(0,0,1,0,1) and φ=(0, π/2, π, -π/2,0); respectively

In order to decode user data, the outputs of both filters have to present temporal alignment previous to the sub-band demodulation process. In particular; for this decoder (address) function the finite rise time of the DTF shown in Figure 5 requires introducing an additional delay line in the filter structure to align both filter responses. Short transmission lines were introduced in the reference filter function for such aim. An inter-stage time compensation of about 15 ps in the first inter-stage delay τ_d (see Figure 2) was needed for this receiver. The late tap was not set to a high gain according with the encoder function (see Figure 5) because this creates large oscillations that affects even more user decoding. We shift all the function phases in Table 1 by +1.1 radians. Inaccuracies associated with time mismatch, finite rise times and high oscillations were reduced.

In order to give an assessment of the filter design method in Section 3, Figure 6 allows making comparisons for two different reference functions used for decoding. This is archived by considering that both the interferer and decoder are referred to the same vector θ_1 or θ_2 (code matching is only shown for θ_1 in that figure). Figure 6 shows results of the decoding achieved by the receiver with address $(0,-\pi/2,\pi,\pi/2,0)$. Code matching and interference rejection are plotted over the same time and frequency scales for comparison proposes. These results are spectral components obtained after mixing the address correlation function with the reference. The inset in Figure 5 shows the time response of the lowpass filter to the mixer output (time scale not shown for clarity). The lowpass filter was designed with a 4th-order Butterworth response with cut-off frequency of 2.0 GHz.

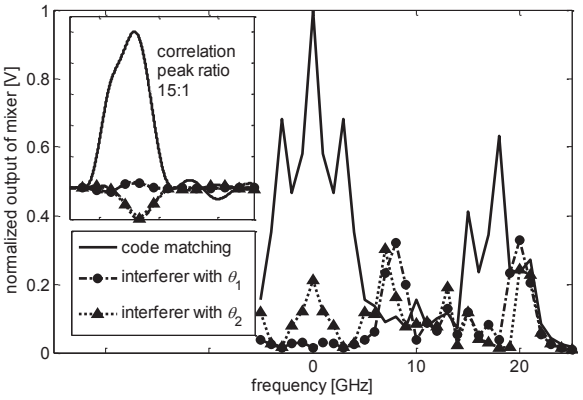

Figure 6 Results of the receiver with address (0,- π/2, π, π/2,0), user (0,0,0,1,1) and one interferer (0,1,0,0,1). Interference rejection is analyzed with reference vectors Θ1=(0, π/2, 0, π/2,0) and Θ2=(0, π/2, π/2, π/2, π/2)

It is seen in Figure 6 that the alternate vector θ_1 provides better interference rejection, providing a correlation peak ratio of 15:1 at the receiver output when compared with the correlation peak for the decoder based on the reference vector θ_2. High correlation peak ratios (not shown herein) were also obtained for the decoder with address vector $(0,-\pi/2,\ 0,-\pi/2,\ 0)$ and all the rest of encoders itemized on Table 1.

The lower interference rejection ratio was obtained for the receiver with address $(0,\pi/2,\pi,-\pi/2,0)$. Results of such function are shown in Figure 7. The alternate vector θ_1 provides a marginal improvement over results based on the selection of θ_2 in both time and frequency responses. The sharp frequency response to the interferer makes the lowpass Butterworth filter unable to filter out large interference. In this case, the correlation peak ratio can be increased if a narrower lowpass filter is used at the mixer output. Additionally, it was confirmed that in other decoding processes in which the rejection band is not as narrower as that shown in Figure 7, the filter method in Section 3 improves consistently the performance of the proposed encoder/decoder structures.

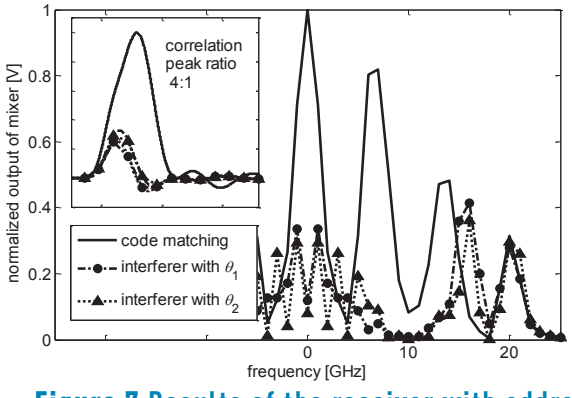

Figure 7 Results of the receiver with address (0, π/2, π, - π/2,0), user (0,1,0,0,1) and one interferer (0,0,1,0,1). Interference rejection is analyzed with reference vectors Θ1=(0, π/2, 0, π/2,0) and Θ2=(0, π/2, π/2, π/2, π/2)

5. Discussion

The encoding method proposed in this paper improves interference rejection margins over previous demonstrations based on DS-CDMA. For instance; when using Gold sequences of length 7 a correlation peak ratio of the order of 2:1 can be obtained theoretically. The method based on decoding unipolar pulses shows a slightly better correlation peak (theoretically a correlation peak ratio of 3:1 [3]). The use of Gold codes of length 7 can create potentially up to 7 quasi-orthogonal channels. However, the processing gain of the CDMA receiver based on the 7-tap DTF is low in comparison with the cross-correlation variance of Gold codes. On the other hand, for a truly asynchronous operation, the cardinality of Optical Orthogonal Codes [10] applied to the DTF method in [3] yields 2 simultaneous users for a cross-correlation peak constrained to 1.

In the proposed encoding method, Hadamard codes of length 4 can provide up to 3 channels. The lower correlation peak obtained by our method was 4:1 for the receiver that shows the larger discrepancies with the (target) waveform. Large correlation peaks is a result of the orthogonality of the used codes and the design of filter functions that allows reducing frequency overlap. In the light of the large interference rejection margins achieved by our CDMA method, it is believed that multi-level codes could increase effectively the number orthogonal or quasi-orthogonal channels negating the need for TF's with large taped delay lines or increased number of filter taps. Computer search of unipolar-bipolar codes can be explored for such aim.

6. Conclusions

This paper introduces a new coding scheme that enables CDMA systems to make use of the analogue processing of DTF's. In order for the filter to be a suitable option, its finite-impulse response must approximate to a noise-like signal which exhibits larger amplitude variations compared with the encoding patterns used in standard DS-CDMA systems. A filter design method was proposed and its suitability was tested using simulation results of DTF´s specifically designed for spectral encoding. The ability to correlating high-speed multilevel pulses by distributed-based transversal filters makes available filter structures that achieve sub-band encoding and decoding. Transient responses were obtained from simulations of monolithic integrated transversal filter implementations at layout level. Advantages of the proposed CDMA system are discussed assuming a single concurrent user in the network showing better correlation peak ratios when compared with those of previous demonstrations based on direct sequence systems.

7. References

1. C. Lam, "To spread or not spread: the myths of optical CDMA", in *13th Annual Meeting of the IEEE Lasers and Electro-Optics Society* (LEOS), Río Grande, Puerto Rico, 2000, pp. 810-811.
2. J. Rosas, J. Ingham, R. Penty and I. White, "18 Gchips/s electronic CDMA for low-cost optical access networks", *Journal of Lightwave Technology*, vol. 27, no. 3, pp. 306-313, 2009.
3. M. Pimenta, "Design and modelling of electronic processing circuits for optical code division multiple access communication networks", Ph.D. thesis, University College London, London, UK, 2009.
4. J. Aguilar and I. Darwazeh, "Dual Drain-line Distributed Cell Design for Multi-Gbit/s Transversal Filter Implementations", in *IEEE International Symposium on Circuits and Systems* (ISCAS), Kobe, Japan, 2005, pp. 3958-3961.
5. L. Chuan-qi *et al.*, "A 10 Gbit/s OCDMA System Based on Electric Encoding and Optical Transmission", *Optoelectronics Letters*, vol. 9, no. 6, pp. 473-476, 2013.
6. M. Kavehrad and D. Zaccarin, "Optical Code-Division-Multiplexed Systems Based on Spectral Encoding of Noncoherent Sources", *Journal of Lightwave Technology,* vol. 13, no. 3, pp. 534-545, 1995.
7. P. Crespo, M. Honig and J. Salehi, "Spread-Time Code-Division Multiple Access", *IEEE Transactions on Communications*, vol. 43, no. 6, pp. 2139-2148, 1995.
8. A. Borjak, P. Monteiro, J. O'Reilly and I. Darwazeh, "High-Speed Generalized Distributed-Amplifier-Based Transversal-Filter Topology for Optical Communication Systems", *IEEE Transactions on Microwave Theory and Techniques,* vol. 45, no. 8, pp. 1453-1457, 1997.
9. J. Aguilar and I. Darwazeh, "Performance analysis of a monolithic integrated transversal filter using mixed-mode scattering parameter", *IET Microwaves, Antennas and Propagation,* vol. 1, no. 4, pp. 925-931, 2007.
10. J. Salehi, "Code-Division Multiple-Access Techniques in Optical Fiber Networks-Part I: Fundamental Principles", *IEEE Transactions on Communications,* vol. 37, no. 8, pp. 824-833, 1989.